Scaling of petiole anatomies, mechanics, and vasculatures with leaf size in the widespread Neotropical pioneer tree species Cecropia obtusa Trécul (Urticaceae)

Sébastien Levionnois, Sabrina Coste, Eric-André Nicolini, Clement Stahl, Hélène Morel, Patrick Heuret

Original Article

Scaling of petiole anatomies, mechanics, and vasculatures with leaf size in the widespread Neotropical pioneer tree species *Cecropia obtusa* Trécul (Urticaceae)

Running title:

Sébastien Levionnois[1*], Sabrina Coste[1], Eric Nicolini[2], Clément Stahl[1], Hélène Morel[1], Patrick Heuret[1,2*]

1. UMR EcoFoG, AgroParisTech, CIRAD, CNRS, INRA, UA, UG, 97379 Kourou Cedex France.
2. UMR AMAP, CIRAD, CNRS, INRA, IRD, Université de Montpellier, 34398 Montpellier, France.

*Authors for correspondence:
Sébastien Levionnois, PhD student
Postal address: UMR EcoFog, Campus Agronomique, Avenue de France
BP709 – 97387 Kourou Cedex
French Guiana
Tel: +33 760 26 73 83
Email: sebastien.levionnois.pro@gmail.com

Patrick Heuret, PhD
Postal adress: UMR AMAP, TA 1-51/PS2 Boulevard de la Lironde
34398 Montpellier Cedex 5
France
Tel: +33 467 61 55 14Email: patrick.heuret@inra.fr

Author contributions

P.H. conceived and designed the study; P.H., S.L., E.N., S.C., H.M. and C.S. collected field samples and measured morphological traits; S.L. performed anatomical sections. S.L. and P.H performed images and data analysis; S.L. and P.H. wrote the manuscript; all authors discussed the results and contributed valuable comments on the manuscript.

ABSTRACT

1. Although the leaf economic spectrum has deepened our understanding of leaf trait variability, little is known about how leaf traits scale with leaf area. This uncertainty has resulted in the assumption that leaf traits should vary by keeping the same pace of variation with increases in leaf area across the leaf size range. We evaluated the scaling of morphological, tissue-surface, and vascular traits with overall leaf area, and the functional significance of such scaling.

2. We examined 1271 leaves for morphological traits, and 124 leaves for anatomical, and hydraulic traits, from 38 trees of *Cecropia obtusa* Trécul (Urticaceae) in French Guiana. *Cecropia* is a Neotropical genus of pioneer trees that can exhibit large laminas (0.4 m^2 for *C. obtusa*), with leaf size ranging by two orders of magnitude. We measured (i) tissue fractions within petioles and their second moment of area, (ii) theoretical xylem hydraulic efficiency of petioles, and (iii) the extent of leaf vessel widening within the hydraulic path.

3. We found that different scaling of morphological trait variability allows for optimisation of lamina display among larger leaves, especially the positive allometric relationship between lamina area and petiole cross-sectional area. Increasing the fraction of pith is a key factor that increases the geometrical effect of supportive tissues on mechanical rigidity and thereby increases carbon-use efficiency. We found that increasing xylem hydraulic efficiency with vessel size results in lower leaf lamina area: xylem ratios, which also results in potential carbon savings for large leaves. We found that the vessel widening is consistent with hydraulic optimisation models.

4. Leaf size variability modifies scaling of leaf traits in this large-leaved species.

Key words: allometry, theoretical hydraulic conductivity, leaf size, petiole anatomy, scaling, vessel widening, xylem.

INTRODUCTION

Leaf traits have received wide attention over recent years because of the major roles they play in the plant carbon economy. A current, widely accepted paradigm exists as part of the global spectrum of leaf economy (LES), which emphasizes the importance of "quick" to "slow" returns on physiological investments (Wright et al. 2004). In this framework, coordination between structural, chemical, and physiological traits has been convincingly described within and between species (Poorter and Evans 1998, Reich et al. 1998, Hikosaka 2004, Shipley et al. 2006, Niinemets 2015, Onoda et al. 2017). Some studies have also investigated some of the anatomical and physiological changes underlying the variability of traits underpinning the LES, such as leaf mass per area (LMA; Scoffoni et al. 2016, John et al. 2017, Onoda et al. 2017). Leaf size (i.e. petiole length and diameter, lamina length, and mainly lamina area), on the other hand, has been generally studied as disconnected from the LES, or has been shown to be decoupled from the LES (Baraloto et al. 2010), although it is a trait that can vary hugely, encompassing six orders of magnitude across vascular plants (Niinemets et al. 2007, Milla and Reich 2007, Wright et al. 2017). For instance, leaf size is certainly subject to strong selective pressures such as light interception (Poorter and Rozendaal 2008, Smith et al. 2017) or temperature regulation (Gates 1968, Parkhurst and Loucks 1972, Leigh et al. 2017). The leaf size – stem size relationship and other related concepts (Corner's rules; (Corner 1949, White 1983a, 1983b, Ackerly and Donoghue 1998); leaf-stem allometry (Brouat et al. 1998, Brouat and McKey 2001, Fan et al. 2017), the leaf size-twig size spectrum (Westoby et al. 2002) and the leptocaulis-pachycaulis spectrum (Hallé et al. 1978)) have been a fruitful framework to tackle the within- and among-species leaf size variability (Westoby et al. 2002), but the related studies remain mainly based on morphological traits (i.e. lamina area, stem cross-sectional area, internode length, petiole length…), rather than anatomical or physiological traits (however see Normand et al. 2008, Fan et al. 2017).

A key aspect of the knowledge gathered from leaf size – stem size relationships, involves crucial questions about how and why leaf size varies across the plant kingdom. The traits expressed in different lamina-petiole functional scaling (i.e. allometric vs isometric) within and between species is likely of significance for these questions. Relationships between two traits x and y can be described as: $y = ax^b$, such as: $\log(y) = \log(a) + b * \log(x)$, where b is the slope (or allometric exponent) and a the intercept (allometric coefficient). An isometric relationship, when $b = 1$, is a linear and proportionality relationship, implying no change of organ or organism form and shape over ontogeny, or across species. An allometric relationship, when $b \neq 1$, is a non-linear and disproportionality relationship, underlying

different pace of variation between two traits, and implying changes of organ or organism form and shape. Discerning allometric vs isometric relationships between organ or organism traits is an important priority, since different functional requirements can be reflected between small vs large organs or organisms, and finally different responses to selective pressures (Harvey and Pagel 1991, Brouat et al. 1998). The lamina-petiole relationship, or the relationship between a given leaf trait with leaf size, has been little studied in this scaling perspective. This gives scattered ideas if leaf size affects leaf functional requirements, and further if sampling both small and large leaves make a big difference for mechanical, hydraulic, and photosynthetic quantifications.

First, a set of studies have argued that larger leaves are disproportionately more carbon expensive, based on the fact that the leaf area fails to keep pace with increases in leaf dry mass, at both inter- (Niinemets et al. 2006, Niklas et al. 2007, Niinemets et al. 2007, Niklas and Cobb 2008, Li et al. 2008, Niklas et al. 2009, Yang et al. 2010) and intraspecific levels (Milla and Reich 2007, Sun Jun et al. 2017). The main explanation is that support requirements increase disproportionately, as the bending moment of a cantilevered beam –as a petiole- scales with the cube of its length (Gere and Timoshenko 1997, Niinemets et al. 2007), in addition to the drag forces applied to the leaf. The leaf mass-leaf area scaling has been relatively little studied at the intraspecific level (Sun Jun et al. 2017). Moreover, the leaf area-petiole cross-sectional area scaling has received less attention. Fan et al. (2017) report an isometric relationship across 28 *Ficus* species. Price and Enquist (2007)'s empirical data support an isometric leaf area-petiole cross-sectional area relationship for 5 out of 18 species, and an allometric relationship for 13 out of 18 species. Finally, for both leaf mass-leaf area and leaf area-petiole cross-sectional area scalings, we do not know the size-related anatomy underlying these scalings.

Mechanical measurements have been applied in relation to leaf area. Studies of Niklas (1991, 1992) and Mahley et al. (2018) demonstrated that small vs large leaves are not mechanically equivalent regarding flexural stiffness, both within and across species, with petioles of large leaves being disproportionately stiffer. But the mechanical structure driving the flexural stiffness between small vs large leaves remains poorly described (Niklas 1999). Mechanical stability can be achieved through two properties: the material property and the geometry. Modification of petiole tissue surfaces and fractions across a leaf size range can determine the mechanical contribution through geometry of main supportive tissues such as xylem, collenchyma, and sclerenchyma (Faisal et al. 2010, Niklas and Spatz 2012). Pith is largely made of large parenchyma cells, and is a cheap due to weak cell wall lignification and

fine cell walls (Evert 2006). As the pith generally occupies the central position within an organ, modifying pith area and fraction could be an efficient way to generate volume with decreased carbon costs (Olson, Rosell, et al. 2018). Moreover, when pith fraction increases, it mechanically shifts external and supportive tissues (xylem, sclerenchyma, collenchyma) centrifugally, increasing the second moment of inertia of theses tissues. Second moment of area quantifies the distribution of mass in a cross-section with respect to the centre of inertia of the cross-section, and this describes the important effect of size and geometry of the cross-section in mechanics. The prevalent role of cross-sectional geometry in the stiffness of petioles has been shown by Mahley et al. (2018), but only for ferns, which exhibit a very different anatomy in comparison to flowering plants.

In comparison to the leaf dry mass-area scaling or petiole mechanics, little is currently known on the link between leaf size, leaf hydraulic conductivity and vascular architecture. Understanding size-related changes of leaf hydraulics and vasculature is important to address size-independent variation, as pointed out for stems (Olson et al. 2009). The West-Brown-Enquist model (WBE model) assumes that the variation of terminal (i.e. minor veins) conduit size and number is independent of leaf size (West et al. 1999, Price and Enquist 2007). Supporting this assumption, Sack et al. (2012) have shown that the global vein density across species is independent of leaf size, even if major vein density decreases with leaf size. Fiorin et al. (2016) suggest that the spatial organisation of stomata with veins is uniform across leaves of different species. But it can also be hypothesised that small vs large leaves across and within species have to deal with different selective pressures regarding conductive path length and the water supply per unit leaf area. Indeed, across the leaf size range, plants should maintain constant leaf conductance per unit leaf area (K_{leaf}, kg MPa^{-1} s^{-1} m^{-2}), or at least minimise the loss of K_{leaf}, to sustain transpiration and carbon assimilation (Petit et al. 2016, Pittermann et al. 2018, Echeverría et al. 2019).

A longer leaf implies *de facto* a longer conductive path length that would thus increase hydraulic resistance and likely affect K_{leaf} in the absence of appropriate vascular adjustments. Theoretical models and empirical data support that the axial basipetal widening in vessel diameter reduces the increase of hydrodynamic resistance with conductive path length (West et al. 1999, Becker et al. 2000, Enquist 2003, Anfodillo et al. 2013, Olson et al. 2014). To our knowledge only two studies measured vessel widening within leaves: Coomes et al. (2008) for ten oak species, and Lechthaler et al. (2019) for one species of *Acer*. Yet, these studies suggest higher rates of vessel widening within leaves, in comparison to stems. This is consistent with the fact that leaves concentrate a significant part of the hydraulic resistance of

the plant (Sack and Holbrook 2006), owing to different vascular architecture between leaves and stems.

A larger leaf also implies *de facto* a larger lamina area to supply with water, and thus an appropriate and sufficient petiole conductivity is required. Increasing the xylem area to increase the number of vessels, or increasing the vessel diameter are two non-exclusive ways of reducing total resistance, and increase petiole and vein conductivity to achieve a sufficient leaf water supply. However, an increase of the number of vessels comes with increasing construction costs, because additional space is required (Banavar et al. 1999, McCulloh et al. 2003, Gleason et al. 2018). The conductivity of a vessel increases with the fourth power of its diameter as predicted by the Hagen-Poiseuille law (Tyree and Zimmermann 2002). Thus, a small increase in vessel diameter will drive an exponential increase in the vessel conductivity, but potentially at the cost of increasing embolism risk. A positive allometric relationship of vasculature with size should increase the xylem conductive efficiency (namely xylem-specific conductivity, which is the xylem conductivity divided by the xylem surface), and therefore should limit xylem volume and construction cost. Investigating the petiole xylem and vasculature according to leaf size can be readily implemented, and should highlight some hydraulic-related selective pressures correlating with the leaf size variability, at both inter- and intraspecific levels.

We chose to investigate lamina-petiole traits at the intraspecific level as a first step. We focussed this study on the genus *Cecropia,* which is known for its hyperdominant pioneer trees that are pivotal in the initiation of tropical forest successions. We selected *Cecropia obtusa* Trécul (Uticaceae), which is a widespread species from the Guiana shield, capable of deploying large leaves with a large size range (100 – 4000 cm^2), appropriate for addressing the lamina-petiole scaling with petiole anatomical and vasculature correlates, at the intraspecific level. We measured leaf morphology, tissue areas of the petiole, petiole vascular and theoretical conductive traits. We built a dataset of 1271 leaves from 38 trees, with anatomical and vascular data for 124 leaves. We aimed to address the following questions:

(i) Is the form of the lamina-petiole scaling isometric or allometric? We hypothesise to find allometric lamina area-petiole cross-sectional area and lamina mass-petiole mass relationships, with petiole mass increasing faster as mechanical requirements disproportionately increase.

(ii) How does petiole anatomy determine petiole mechanics? We hypothesise that pith fraction increases with leaf size, minimising volumetric construction cost, and enhancing mechanical strength through geometry by shifting supportive tissues centrifugally.

(iii) How do longitudinal adjustments of xylem and vasculature variations limit loss of K_{leaf} and construction costs? We hypothesise that K_{leaf} loss limitation for larger leaves is allowed by vessel basipetal widening according to the leaf size and the conductive path length. We hypothesise to find a higher rate of vessel widening within the leaf in comparison to what is known for the stem, consistent with leaves supporting a large amount of the total hydraulic resistance of plants. We also hypothesise that less construction cost is possible than under the hypothesis of an invariable vessel diameter, thanks to a more efficient xylem due to wider vessels, enabling more lamina area per xylem area.

MATERIALS AND METHODS

Study site

The study was conducted in French Guiana along a forestry road in Counami (N5.41430°, W53.17547°, geodesic system WGS84) where the entrance to the road is located 5 km to the east of Iracoubo municipality. The warm wet tropical climate of French Guiana is highly seasonal due to the north-south movement of the Inter-Tropical Convergence Zone. Mean annual rainfall is 2726 mm $year^{-1}$ and annual mean air temperature is 25.7 °C (Gourlet-Fleury et al. 2004). There is a dry season lasting from mid-August to mid-November, during which rainfall is < 100 mm $month^{-1}$.

Plant material, sampling and morphological measurements

Tree sizes ranged from 10.8 to 23.1 m in height, and 6.21 to 30.49 cm in diameter at breast height. Trees were evenly felled in time from September 2014 to October 2016. All the leaves in the crown were cut by cutting the petiole as close as possible to its insertion point with the stem and placed immediately in plastic bags within coolers. One to five fully expanded leaves per tree -hereafter called A-leaves - were kept for the anatomical studies.

Cecropia leaves are palmatilobate (Fig. 1b; Fig. S1) and so there is no single midrib but the same number of midribs as there are lobes, i.e. a midrib departs into and supplies each lobe. In the laboratory, all the leaves were processed within 4 hours after felling to keep them as fresh as possible. Petioles were cut as close to the lamina as possible. Two orthogonal diameters (mm) of each petiole, at the middle point of the petiole, were measured because of the tendency of *Cecropia* petioles to exhibit an ellipse shape (Fig. S1; Table 1 for a list of traits and abbreviation). From these two diameters, a cross-sectional area was derived in the shape of an ellipse (A_{pet}, mm^2; Fig. S1). For each lamina, the length of the main lobe (i.e. the largest one in the continuation of the petiole; cm) was measured. In the A-leaves, two 1-cm-

long petiole segments in the median position was sampled (Fig. S1). The first segment was used to measure their specific density, expressed as the ratio of dry mass to the fresh volume (PD: petiole density; Williamson and Wiemann 2010; Table 1). The fresh volume of the sample was calculated using an inverse Archimedes principle and a precision balance (CP224S, Sartorius), based on the buoyancy (G) of the sample, i.e. G = fresh mass in air – submerged mass (Lehnebach et al. 2019). Dry mass was derived after drying at 103 °C for three days. PD was computed as the dry mass divided by G. The second segment was preserved in 70% alcohol and used later for anatomical measurements (see the section headed '*Anatomical measurements*'). Because we aimed at studying the effects of the fraction and cross-sectional area of petiole tissues, we choose to focus on the mid-point segment of the petiole between the connection to the stem and the leaf lamina. This point was selected so as to avoid swelling effects at stem and lamina connections. At the base of the petiole, the wide and triangular base is further modified by an external covering of trichilia and secretions of Müllerian bodies serving the nutrition of hosted ants. At the distal end of the petiole, at the point of junction between petiole and lamina main veins, the petiole is more flexible in torsion, which allows the lamina to rotate (pers. obs.). The distance between the anatomical sampling point and the tip of the leaf main lobe was measured (conductive path length; PL, cm) and used for the investigation of vessel widening. Since the vessel diameter – conductive path length relationship is a power function, with rapid changes in vessel diameters close to the conductive path tip, and slower nearly constant toward the base, we assume that anatomical measurements at our sampling point are proportional to the petiole base.

Lamina dry mass (M_{lamina}, g) and petiole dry mass (M_{pet}, g) were measured with a scale. The leaf dry mass (M_{leaf}, g) is the sum of M_{lamina} and M_{pet}. Lamina area (A_{lamina}, cm²; Fig. S1) was measured with a planimeter (LiCor 3000A, LiCor Inc., Lincoln, NE, USA).

Data from 1271 mature fully developed leaves (A-leaves and all the other leaves) were used for the characterisation of morphological and structural variability.

Anatomical and vascular measurements

We conducted our study on a subset of 124 A-leaves selected to represent the widest range of petiole diameters (from 2.56 to 15.41 mm). Anatomical cross-sections (Fig. 1c), 20 to 50 µm thick, were sampled from the petiole median segment with a manual microtome (Mikrot L, Schenkung Dapples, Switzerland). All cross-sections were stained in a safranin/astra-blue solution to stain unlignified cells blue and lignified cells red. Images of each petiole cross-section were digitised with an optical microscope (Olympus BX60; Olympus Corporation;

Tokyo; Japan) with 50x magnification and a Canon camera EOS 500D (lens Olympus U-TVI-X ; F 0.0; ISO 100; speed 1/25). Three or four close up images were taken of each petiole section at different depths of focus and stacked with the Helicon Focus software (v.6.3.2.Pro, https://www.heliconsoft.com/). Pictures were assembled in a panorama using Kolor AutoPanoGiga software (v.3.0.0, http://kolor.com/autopano/) to obtain a complete picture of the cross-section (Fig. 1c). The digitised cross-sections were processed with CS5 Photoshop software (v.12.0, http://adobe.com/products/photoshop/html). We distinguished eight tissue types that comprise the entire petiole anatomy (Fig. 1d, e). We manually delineated the tissues on the photographs and created layer masks (Fig. 1e). The masks of these layers were used to calculate the cross-sectional area of each tissue and the whole petiole cross-sectional area with the ImageJ software (v.1.43u; http://imagej.nih.gov/ij/). We distinguished eight component petiole tissues for further anatomical analysis: (i) the pith, (ii) the sclerenchymatous shield associated with the vascular bundles, (iii) interfascicular parenchyma, (iv) primary xylem, (v) secondary xylem, (vi) phloem (comprising primary and secondary phloem), (vii) cortical parenchyma and (viii) cortical collenchyma (Fig. 1e).

As we knew the cross-sectional area of each petiole tissue, we calculated the second moment of area (I, mm^4) of the main supportive tissues (Table 1). I quantifies the distribution of mass in a cross-section with respect to the centre of mass of the cross-section, and this describes the important effect of size and geometry of the cross-section in mechanics, since the flexural stiffness ($E*I$, where E is the elastic modulus) is directly proportional to I (Niklas and Spatz 2012). As I is a fourth power function of the two radii delimiting the ring (Table 1), slight increases in the ring diameter and/or cross-sectional area has dramatic consequences for I, and thus its contribution to flexural stiffness. We focused on the sclerenchyma, collenchyma and secondary xylem, since these tissues are well-known to be supportive tissues in a section and exhibit lignified thick cell walls (Leroux 2012). We also estimated the behaviour of the petiole flexural stiffness by calculating I for the total petiole section, and by using the known petiole density as a proxy of E (Table 1). We assumed that this approximation was appropriate, since it had been shown that the elastic modulus exhibits a linear and positive relationship with the density for both wood (Chave et al. 2009, Dlouhá et al. 2018) and bark (Rosell and Olson 2014).

For the xylem, the cropped part of the image in which the vessels were visible was analysed with the ImageJ software to calculate theoretical xylem hydraulic properties (Abramoff et al. 2004). For each vessel, we calculated its cross-sectional area (μm^2) and its elliptical diameters. To study variations in the dimensions of the vessel, we used the mean

hydraulic diameter (D_h, µm, Table 1), i.e. the diameter that all vessels, considered as circles, in a given tissue would have to sustain exactly the same tissue hydraulic conductivity (Tyree and Zimmermann 2002). The number of vessels was counted for primary and secondary xylem. We also calculated the conductive area (mm²) as the sum of the cross-sectional area of all vessels of the surrounding xylem. Knowing the dimensions of each vessel, the number of vessels, and the total petiole xylem area, a theoretical hydraulic conductivity (K_{th}, m kg MPa^{-1} s^{-1}) was estimated based on formulas in Table 1. To test the null hypothesis of a decreasing K_{leaf} (kg MPa^{-1} s^{-1} m^{-2}) across the leaf size range with no vessel widening occurring, we estimated a theoretical leaf conductance ($K_{leaf,null}$) by firstly dividing the K_{th} by the petiole length. We thus obtained a value for petiole conductance (kg MPa^{-1} s^{-1}) which we divided by the lamina area and obtaining $K_{leaf,null}$.

Previous studies have shown precise tapering rates of vessels along a leaf (Coomes et al. 2008; Lechthaler et al. 2019) or the entire tree (Bettiati et al. 2012, Petit et al. 2014) based on several anatomical measurements along the path of each individual leaf or individual tree. Here, we estimated a tapering rate (D_h/PL) based on a scaling exponent of the log-log relationship between D_h at the midpoint of the petiole, and the path length, across all measured petioles. Following past studies at the tree level for interspecific comparisons (Anfodillo et al. 2006; Olson et al. 2014), we assumed that vessel tapering is primarily determined by the distance from the leaf tip, assuming that all leaves display the same tapering rate.

Data analysis

Laminas used in anatomical studies were sometimes slightly damaged resulting in somewhat biased lamina area measurements. To correct this, we used a prediction model to calculate an estimated lamina area (A_{lamina}, cm²), since the relationship between the length of the main lobe and the undamaged lamina area is very informative. We calculated the estimated lamina area as: $Estimated\ lamina\ area = 0.701 * Main\ lobe\ length^{2.180}$ ($R^2 = 0.942$, $P < 0.001$, Fig. S2). This estimation of lamina area was used only to compare tissue cross-sectional area and vasculature traits with leaf area.

All statistical analyses were performed with R software (https://cran.r-project.org/). The relationship between each trait pair was determined with an SMA (Standardized major axis regression; Warton et al. 2006), which allows minimisation of the error on both the *x*-axis and *y*-axis (Harvey and Pagel 1991). These correlation relationships are described as: $y = ax^b$, such as: $\log(y) = \log(a) + b * \log(x)$, where *b* is the slope (or allometric exponent) and *a* the

intercept (allometric coefficient). A 95% confidence interval was used to decide whether it was significantly correlated or not. A slope test was performed to determine if the slope differed from 1 (H1: b ≠ 1 for an allometric relationship) or not (H0: b = 1 for an isometric relationship). SMA were carried out with the (S)MATR package (Falster et al. 2006). The lamina area prediction from the main lobe length was modelled from a NLS (non-linear least squares) with the STATS package.

RESULTS

Leaf morphological variability

A_{pet} and A_{lamina} were positively and allometrically correlated ($P < 0.001$; $R^2 = 0.779$; Fig. 2a; Table 2, S1). A_{pet} and M_{lamina} were positively, and allometrically correlated ($P < 0.001$; $R^2 = 0.898$; Fig. 2b; Table 2). M_{pet} and M_{lamina} were positively, and allometrically correlated ($P < 0.001$; $R^2 = 0.947$; Fig. 2c; Table 2). A_{lamina} and M_{leaf} were positively, and isometrically correlated ($P < 0.001$; $R^2 = 0.846$; Fig. 2d; Table 2). PD were negatively, and allometrically correlated to A_{pet} ($P < 0.01$) but uncorrelated to A_{lamina} ($P < 0.05$)(Table S1).

Petiole anatomy

Petioles showed pronounced radial symmetry (Fig. 1c). The central parenchymatous pith formed the main part of the cross-section. The numerous bundles (20 to 80) were arranged in the pith periphery, mainly in only one circle, but in a few cases in two circles. The cambium displayed a diversity of arrangement, with respect to the arrangement of the bundles. From a strictly cyclic structure to a wavy one (Fig. 1f), and at the extremity, we observed isolated bundles with complete cambium discontinuities in a more cortical position (Fig. 1g). Primary and secondary xylem and secondary phloem were easy to identify (Fig. 1d). A sub-continuous sclerenchymatous shield was present at the interface between the vascular bundles and the pith. The vascular bundles were separated by interfascicular parenchyma. Occasional sclerenchyma were present between the secondary phloem and cortical parenchyma. Depending on the extent of secondary growth, the primary phloem was crushed between the secondary phloem and cortical parenchyma. In the most external part, there was a ring of collenchyma, between the epidermis and the cortical parenchyma. Laticiferous canals were frequently visible, mainly in the cortex (Fig. 1f) but also in the pith, but were also sometimes completely absent.

Petiole anatomy and vascular architecture

All tissue areas were significantly and positively correlated with A_{pet} and A_{lamina} ($P < 0.001$; Fig. S3a; Table S2), with most of these relationships being allometric. All tissue fractions relative to A_{pet} were correlated to A_{pet} ($P < 0.001$; Fig. S3b; Table S2). All tissue fractions relative to A_{pet} were correlated to A_{lamina} ($P < 0.001$; Fig. S3b; Table S2), except for the phloem ($P > 0.05$). Pith had the highest fraction (44.78% ± 1.12) with the highest effect on petiole size (27.02 to 59.41% of the cross-section; Fig. 3a). The lamina area allometrically and positively scaled with the number of vessels ($P < 0.001$; $R^2 = 0.596$; Fig. 3d; Table 2), such that large leaves were associated with disproportionately less vessels. The lamina area allometrically and positively scaled with conductive area ($P < 0.001$; $R^2 = 0.635$; Fig. 3c; Table 2), such that large leaves were associated with disproportionately less conductive area. The lamina area allometrically and positively scaled with xylem area ($P < 0.001$; $R^2 = 0.711$; Fig. 3b; Table 2), such that large leaves were associated with disproportionately less xylem area.

The second moment of area (*I*) for collenchyma, secondary xylem, and sclerenchyma were significantly and positively related to A_{lamina} ($P < 0.001$; $R^2 = 0.578$, 0.712, and 0.645 respectively; Fig. 4a,b,c). The approximated petiole flexural stiffness was positively and allometrically correlated to A_{lamina} with a slope significantly superior to 1 ($P < 0.001$; $R^2 = 0.653$; Fig. 4d; Table 2).

D_h was significantly and positively related to A_{lamina} ($P < 0.001$; $R^2 = 0.502$; Fig. 5a; Table 2). D_h was positively and allometrically related to the conductive path length ($P < 0.001$; $R^2 = 0.469$; Fig. 5b; Table 2). The estimated tapering rate (D_h/PL) was 0.549 µm cm^{-1} (Fig. 5b). $K_{leaf,null}$ was significantly and negatively related to A_{lamina} and the conductive path length ($P < 0.01$; Fig. 5c,d).

DISCUSSION

Our results provide an understanding of the tissue-level and vascular adjustments characterising lamina-petiole scaling at the intraspecific level for a widespread Neotropical pioneer tree species, *Cecropia obtusa*. The results point out (i) an allometric scaling between lamina size and petiole size, such that larger leaves show a higher lamina area for a given petiole cross-section, (ii) a higher pith fraction, related to higher petiole flexural stiffness through the second moment of area (*I*) of the mechanically stiff tissues surrounding the pith, (iii) a vessel widening allowing for a reduced effect of increasing path length with leaf size and (iv) a higher lamina area per xylem area for larger leaves, due to relatively less conductive area for larger leaves.

Morphological petiole-lamina scaling

The finding of a positive and allometric relationship between petiole dry mass and lamina dry mass (Fig. 2c), with a disproportionately higher petiole mass for a given lamina mass, is in agreement with what has been previously described (Niinemets et al. 2006, 2007, Li et al. 2008). This pattern has been explained by the scaling of the bending moment of a cantilevered beam with the cube of its length (Gere and Timoshenko 1997), in addition to drag forces requiring a disproportionate mechanical reinforcement of the petiole with leaf size (Niinemets et al. 2007, Li et al. 2008). However, the isometric scaling of lamina area with the leaf dry mass (Fig. 2d) is not in agreement with the repeatedly shown diminishing return pattern, predicting increasing costs for leaf support with increasing leaf size (Niinemets et al. 2006, 2007, Niklas et al. 2007, 2009, Milla and Reich 2007, Li et al. 2008b, Sun Jun et al. 2017). Although the leaf area-leaf mass allometric scaling is significant at the interspecific level, the allometric scaling is not ubiquitous at the intraspecific level, based on this present study for *C. obtusa*, and Milla and Reich (2007) for 11 species.

We found a positive allometric relationship between lamina area and petiole cross-sectional area (Fig. 2a), such that large leaves exhibit a larger lamina area for a given petiole cross-sectional area. This change is in agreement with the allometric relationship between lamina mass and petiole cross-sectional area we found (Fig. 2b), such that large leaves exhibit larger lamina mass for a given petiole size. Larger petioles support a disproportionately larger load. Therefore, we wondered what petiole anatomical and mechanical changes are associated with this morphological pattern.

Petiole tissue partitioning

As pith fraction increases, the distance of a given tissue to the petiole cross-sectional centre of inertia increases, as does the second moment of inertia to a fourth-power function of this distance. The case of collenchyma is of primary importance since it is known to be a supporting tissue, with small cells and relatively thick cell walls compared with other living cells (Leroux 2012). The collenchyma is the most external tissue within the petiole section with a ring-geometry, exhibiting the largest change in the second moment of area (Fig. 4a). In the same line, the secondary xylem is also a well-known supporting tissue, exhibiting a ring-geometry and which fraction increases with leaf size. Its increasing fraction occurs at the same time as the distance to the cross-sectional centre of inertia increases with pith fraction, and determines an overall increase of the second moment of area of the secondary xylem with

leaf size (Fig. 4b). This was also the case for the sclerenchyma (Fig. 4c), although sclerenchyma exhibited relatively low values of I (0.05 to 95 mm^4). The allometric exponents of the supportive tissues according to the lamina area (Fig. 4a,b,c) indicate that I increases faster for the sclerenchyma, followed by the secondary xylem, suggesting that the relative geometrical contribution of these tissues to the petiole flexural stiffness increases across the leaf size range.

Increasing organ size and mass logically increases the mechanical load (Mahley et al. 2018). Moreover, we found an allometric relationship between lamina dry mass and petiole cross-sectional area, with disproportionately higher lamina dry mass for leaves (Fig. 2b). This suggests a disproportionately higher mechanical load on petioles of large leaves. This is in agreement with the approximated petiole flexural stiffness allometrically related to the lamina area (Fig. 4d), such that petioles are disproportionately stiffer on large leaves to overcome the mechanical load. This suggestion is in agreement with past studies demonstrating disproportionately higher petiole stiffness with increasing petiole thickness (Niklas 1991, 1992, Mahley et al. 2018). Therefore, our results suggest that the effect of geometry through pith fraction determines the overall increase in petiole flexural stiffness, since the decrease of petiole density with leaf size –and thus petiole elastic modulus- is balanced (Fig. 4d), as also shown by Mahley et al. (2018) for ferns. However, since the pith is often hollow in large structure, one may not exclude that the pressure of selection is actually on the surrounding tissues.

Changing petiole pith fraction and thus collenchyma, secondary xylem, and sclerenchyma I is clearly a cheap mechanism in terms of carbon allocation to balance the self-loading mechanical stress arising with leaf size. Moreover, we found a negative relationship between A_{pet} and PD, and no relationship of PD with A_{lamina}. These results suggest that volumetric construction cost can decrease with A_{pet}, or at least does not increase with leaf size.

Petiole vascular architecture

The estimation of $K_{leaf,null}$ (Fig 5a,b) confirms that K_{leaf} decreases with leaf size in the case of an absence of vessel widening, as the hydraulic resistance is well-known to be dependent on the path length (Tyree and Zimmermann 2002). Without vessel widening, large leaves cannot be selected since (i) the higher pressure drop that would be associated with such leaves would increase the risk of cavitation (Tyree and Ewers 1991, Cruiziat et al. 2002), and (ii) a lower K_{leaf} necessarily drives lower gas exchanges and carbon assimilation (Brodribb 2009, Scoffoni et al. 2016), and thus less efficient carbon payback. Therefore, this result suggests that K_{leaf} is

constant across leaves and not limiting for carbon assimilation (Echeverría et al., Petit et al. 2016, Pittermann et al. 2018), even if water flux measurements would be required for confirmation.

Even if such a pattern of vessel widening has been repeatedly shown along the stem of adult trees for several species (Petit et al. 2008, 2010, Bettiati et al. 2012, Anfodillo et al. 2013, Olson et al. 2014), leaves have received less attention. The estimated widening rate (0.55) was closely similar to those found by Coomes et al. (2008; mean of 0.54; a range of 0.42-0.73) across ten *Quercus* L. (Fagaceae) species, and not too far from those found by Lechthaler et al. (2019; slope of 0.45) for one species of *Acer*. A striking feature here is the convergence of widening rates between studies, despite contrasting ecology (i.e. temperate vs tropical) and phylogenetic origins of the investigated species. Such a finding suggests that the hydrodynamic resistance is such a strong selective pressure on hydraulic architecture that it drives a single leaf vascular architecture across vascular plants. Hydraulic optimality models (West et al. 1999) predict a minimum and convergent widening rate of 0.2, but only for stems, to totally mitigate the hydrodynamic resistance. Indeed, this convergent widening rate is found across most plants and trees when looking into the stem vasculature (Anfodillo et al. 2006, 2013, Petit et al. 2014, Olson et al. 2014, 2018). The vessel widening rate is not constant through the total path length (Bettiati et al. 2012), with a scaling 2 to 3 times higher in leaves (this study; Coomes et al. 2008, Lechthaler et al. 2019). This participates at concentrating much of the hydraulic resistance in leaves –up to 50%- (Sack and Holbrook 2006), whereas leaves represent a small fraction of the total conductive path length, i.e. few centimetres of few tens of centimetres for leaves against tens of meters for the entire tree. The hydraulic segmentation hypothesis (Tyree and Zimmermann 2002, Pivovaroff et al. 2014) assumes that leaves should be hydraulically more resistant than stems, as "bottlenecks", to always preserve far lower water potentials in leaves, and promote drought-induced embolism containment in easy-to-renew organs. These issues deserve more investigations, to link vessel widening rates in leaves with the relative contribution of leaves in the hydraulic resistance of plants.

The allometric relationship between the number of vessels and the supplied lamina area suggests an increase in the number of vessels per leaf area, from the leaf base towards the leaf tip (Fig. 3d). This therefore suggests vessel furcation. This contradicts the WBE model (West et al. 1999, Rosell et al. 2017) which predicts an absence of furcation, even if the WBE model does not initially integrate predictions for leaves. However, this result is in agreement

499 with the empirical test of Lechthaler et al. (2019), who also support the existence of conduit
500 furcation towards terminal parts within *Acer* leaves.

501 For *C. obtusa* leaves, vessel tapering and furcation towards the leaf tip leads to a
502 conductive area-decreasing architecture towards the leaf base, as supported by the allometric
503 relationship between the conductive area and the supplied lamina area (Fig. 3c). This supports
504 the prediction of the WBE model (West et al. 1999, Rosell et al. 2017). However, our result is
505 not in agreement with Lechthaler et al. (2019), who support a conductive area-preserving
506 architecture for *Acer* leaves. This discrepancy may come from the fact that Lechthaler et al.
507 (2019) analysed the vascular architecture across both the petiole and the midrib, whereas in
508 our study we only focused on the petiole. In the lamina, the strong furcation of the vein
509 system may lead to more numerous vessel furcations in comparison with the petiole.
510 Therefore, less vessel furcations within the petiole may allow for wider vessels, therefore
511 reducing the required conductive area, according to the Hagen-Poiseuille law.

512 The conductive area-decreasing architecture allows for a reduction of the xylem area
513 supplying the lamina for large leaves, as supported by the allometric relationship between
514 xylem area and lamina area (Fig. 3b). According to the Hagen-Poiseuille's law, a given
515 conductive area can determine different conductivities, from numerous but small conduits to
516 few but wide conduits. However, according to the packing rule, the building of numerous
517 small conduits would require more xylem area and volume. Therefore, this implies that
518 selection favours an even water supply to all parts of the leaf independently of leaf size, with
519 minimal carbon investment (Banavar et al. 1999).

520 Finally, disproportionately less xylem area for large leaves explains the allometric
521 relationship between the petiole cross-sectional area and the lamina area, with
522 disproportionately less petiole cross-sectional area for large leaves.

523

524 **CONCLUSION**

525 The different functional attributes linking flexural stiffness (elastic modulus vs *I*, and
526 allometric scaling of flexural stiffness), carbon cost (leaf mass and density), and vasculature
527 (vessel widening, xylem area, and conductive area) between large and small leaves, suggest
528 that these three functional dimension –mechanics, carbon allocation, and hydraulics
529 respectively- are selected for precise combinations, and further determine leaf size variation
530 possibilities. Environmental factors are known to shape leaf size diversity (e.g. annual
531 rainfall, temperature, solar radiation, soil nutrients…), but some other selective pressures are
532 intrinsically linked to the possibility of developing large leaves or not (i.e. return on invested

biomass, self-loading, conductive path length…). The contrasting mechanics, carbon allocation, and vasculatures between large and small leaves shed light on these selective pressures in our study. Indeed, we showed that large leaves exhibited (i) disproportionately higher lamina area for a given petiole cross-sectional area, (ii) higher pith fraction with disproportionately stiffer petioles, and (iii) disproportionately less xylem area for a given lamina area, associated with a decreasing-area vascular architecture toward the leaf base. But these selective pressures are currently not fully understood. Our study calls for more studies on these selective pressures to better characterise and understand to what extent they are independent or not. We argue that a better comprehension of these selective pressures should extend the knowledge of drivers shaping leaf size variability, and, furthermore, permit us to understand how and why leaf size seems disconnected from LES.

ACKNOWLEDGEMENTS

The authors thank Julie Bossu, Coffi Belmys Cakpo, Henri Caron, Jocelyn Cazal, Saint-Omer Cazal, Aurélie Cuvelier, Bruno Clair, Aurélie Dourdain, Jean-Yves Goret, Marie Hartwig, Ariane Mirabel, Audin Patient, Pascal Petronelli, Laurent Risser, Dylan Taxile, Valérie Troispoux, Niklas Tysklind and Lore Verryckt for their assistance with field work and measurement of leaf traits. We thank Jacques Beauchêne, Christine Heinz and Nick Rowe for preliminary discussions around the project and first results. We thank Hervé Cochard for fruitful discussions for data analysis. We thank Tancrède Alméras, Camilo Zalamea and Nick Rowe for critical and valuable comments on successive version of the manuscript.

FUNDING

S.L. was supported by a doctoral fellowship from CEBA (ref. ANR-10-LABX-0025). This study benefited from an *Investissement d'Avenir* grant managed by the *Agence Nationale de la Recherche* (CEBA, ref. ANR-10-LABX-0025).

LITERATURE CITED

Abramoff MD, Magalhães PJ, Ram SJ (2004) Image processing with ImageJ. Biophotonics Int 11:36–42.

Ackerly D, Donoghue MJ (1998) Leaf size, sapling allometry, and Corner's rules: phylogeny and correlated evolution in maples (Acer). Am Nat 152:767–791.

Anfodillo T, Carraro V, Carrer M, Fior C, Rossi S (2006) Convergent tapering of xylem conduits in different woody species. New Phytol 169:279–290.

Anfodillo T, Petit G, Crivellaro A (2013) Axial conduit widening in woody species: a still neglected anatomical pattern. IAWA J 34:352–364.

Banavar JR, Maritan A, Rinaldo A (1999) Size and form in efficient transportation networks. Nature 399:130.

Baraloto C, Timothy Paine CE, Poorter L, Beauchene J, Bonal D, Domenach A-M, Hérault B, Patiño S, Roggy J-C, Chave J (2010) Decoupled leaf and stem economics in rain forest trees. Ecol Lett 13:1338–1347.

Becker P, Gribben RJ, Lim CM (2000) Tapered conduits can buffer hydraulic conductance from path-length effects. Tree Physiol 20:965–967.

Bettiati D, Petit G, Anfodillo T (2012) Testing the equi-resistance principle of the xylem transport system in a small ash tree: empirical support from anatomical analyses. Tree Physiol 32:171–177.

Brodribb TJ (2009) Xylem hydraulic physiology: The functional backbone of terrestrial plant productivity. Plant Sci 177:245–251.

Brouat C, Gibernau M, Amsellem L, McKey D (1998) Corner's Rules revisited: ontogenetic and interspecific patterns in leaf-stem allometry. New Phytol 139:459–470.

Brouat C, McKey D (2001) Leaf-stem allometry, hollow stems, and the evolution of caulinary domatia in myrmecophytes. New Phytol 151:391–406.

Chave J, Coomes D, Jansen S, Lewis SL, Swenson NG, Zanne AE (2009) Towards a worldwide wood economics spectrum. Ecol Lett 12:351–366.

Coomes DA, Heathcote S, Godfrey ER, Shepherd JJ, Sack L (2008) Scaling of xylem vessels and veins within the leaves of oak species., Scaling of xylem vessels and veins within the leaves of oak species. Biol Lett Biol Lett 4, 4:302, 302–306.

Corner EJH (1949) The Durian Theory or the origin of the modern tree. Ann Bot 13:367–414.

Cruiziat P, Cochard H, Améglio T (2002) Hydraulic architecture of trees: main concepts and results. Ann For Sci 59:723–752.

Dlouhá J, Alméras T, Beauchêne J, Clair B, Fournier M (2018) Biophysical dependences among functional wood traits. Funct Ecol 32:2652–2665.

Echeverría A, Anfodillo T, Soriano D, Rosell JA, Olson ME (2019) Constant theoretical conductance via changes in vessel diameter and number with height growth in Moringa oleifera. J Exp Bot 70:5765–5772.

Enquist B (2003) Cope's Rule and the evolution of long-distance transport in vascular plants: allometric scaling, biomass partitioning and optimization. Plant Cell Environ 26:151–161.

Evert R (2006) Parenchyma and Collenchyma. In: Esau's Plant Anatomy. Wiley-Blackwell, pp 175–190.

603 Faisal TR, Khalil Abad EM, Hristozov N, Pasini D (2010) The impact of tissue morphology,
604 cross-section and turgor pressure on the mechanical properties of the leaf petiole in
605 plants. J Bionic Eng 7:S11–S23.

606 Falster DS, Warton DI, Wright II (2006) User's guide to SMATR: Standardised Major Axis
607 tests & routines Version 2.0, Copyright 2006. R Instr

608 Fan Z-X, Sterck F, Zhang S-B, Fu P-L, Hao G-Y (2017) Tradeoff between stem hydraulic
609 efficiency and mechanical strength affects leaf–stem allometry in 28 Ficus tree
610 species. Front Plant Sci 8

611 Fiorin L, Brodribb TJ, Anfodillo T (2016) Transport efficiency through uniformity:
612 organization of veins and stomata in angiosperm leaves. New Phytol 209:216–227.

613 Gates DM (1968) Transpiration and leaf temperature. Annu Rev Plant Physiol 19:211–238.

614 Gere JM, Timoshenko SP (1997) Mechanics of materials. PWS Publishing Company, Boston.

615 Gleason SM, Blackman CJ, Gleason ST, McCulloh KA, Ocheltree TW, Westoby M (2018)
616 Vessel scaling in evergreen angiosperm leaves conforms with Murray's law and area-
617 filling assumptions: implications for plant size, leaf size and cold tolerance. New
618 Phytol 218:1360–1370.

619 Gourlet-Fleury S, Guehl JM, Laroussine O (2004) Ecology and management of a neotropical
620 rainforest : lessons drawn from Paracou, a long-term experimental research site in
621 French Guiana. Elsevier, Paris.

622 Hallé F, Oldeman RAA, Tomlinson PB (1978) Tropical Trees and Forests - An Architectural
623 Analysis. Springer-Verlag Berlin Heidelberg.

624 Harvey PH, Pagel MD (1991) The comparative method in evolutionary biology. Oxford
625 University Press.

626 Hikosaka K (2004) Interspecific difference in the photosynthesis–nitrogen relationship:
627 patterns, physiological causes, and ecological importance. J Plant Res 117:481–494.

628 John GP, Scoffoni C, Buckley TN, Villar R, Poorter H, Sack L (2017) The anatomical and
629 compositional basis of leaf mass per area. Ecol Lett 20:412–425.

630 Lechthaler S, Colangeli P, Gazzabin M, Anfodillo T (2019) Axial anatomy of the leaf midrib
631 provides new insights into the hydraulic architecture and cavitation patterns of Acer
632 pseudoplatanus leaves. J Exp Bot.

633 Lehnebach R, Bossu J, Va S, Morel H, Amusant N, Nicolini E, Beauchêne J (2019) Wood
634 density variations of legume trees in french guiana along the shade tolerance
635 continuum: heartwood effects on radial patterns and gradients. Forests 10:80.

636 Leigh A, Sevanto S, Close JD, Nicotra AB (2017) The influence of leaf size and shape on leaf
637 thermal dynamics: does theory hold up under natural conditions? Plant Cell Environ
638 40:237–248.

639 Leroux O (2012) Collenchyma: a versatile mechanical tissue with dynamic cell walls. Ann
640 Bot 110:1083–1098.

641 Li G, Yang D, Sun S (2008a) Allometric relationships between lamina area, lamina mass and
642 petiole mass of 93 temperate woody species vary with leaf habit, leaf form and
643 altitude. Funct Ecol 22:557–564.

644 Li G, Yang D, Sun S (2008b) Allometric relationships between lamina area, lamina mass and
645 petiole mass of 93 temperate woody species vary with leaf habit, leaf form and
646 altitude. Funct Ecol 22:557–564.

647 Mahley JN, Pittermann J, Rowe N, Baer A, Watkins JE, Schuettpelz E, Wheeler JK,
648 Mehltreter K, Windham M, Testo W, Beck J (2018) Geometry, allometry and
649 biomechanics of fern leaf petioles: their significance for the evolution of functional
650 and ecological diversity within the Pteridaceae. Front Plant Sci 9

651 McCulloh KA, Sperry JS, Adler FR (2003) Water transport in plants obeys Murray's law.
652 Nature 421:939.

653 Milla R, Reich PB (2007) The scaling of leaf area and mass: the cost of light interception
654 increases with leaf size. Proc R Soc Lond B Biol Sci 274:2109–2115.

655 Niinemets Ü (2015) Is there a species spectrum within the world-wide leaf economics
656 spectrum? Major variations in leaf functional traits in the Mediterranean sclerophyll
657 Quercus ilex. New Phytol 205:79–96.

658 Niinemets Ü, Portsmuth A, Tena D, Tobias M, Matesanz S, Valladares F (2007) Do we
659 underestimate the importance of leaf size in plant economics? Disproportional scaling
660 of support costs within the spectrum of leaf physiognomy. Ann Bot 100:283.

661 Niinemets Ü, Portsmuth A, Tobias M (2006) Leaf size modifies support biomass distribution
662 among stems, petioles and mid-ribs in temperate plants. New Phytol 171:91–104.

663 Niklas KJ (1991) Flexural stiffness allometries of angiosperm and fern petioles and rachises:
664 evidence for biomechanical convergence. Evolution 45:734–750.

665 Niklas KJ (1992) Petiole mechanics, light interception by Lamina, and "Economy in Design".
666 Oecologia 90:518–526.

667 Niklas KJ (1999) A mechanical perspective on foliage leaf form and function. New Phytol
668 143:19–31.

669 Niklas KJ, Cobb ED (2008) Evidence for "diminishing returns" from the scaling of stem
670 diameter and specific leaf area. Am J Bot 95:549–557.

671 Niklas KJ, Cobb ED, Niinemets Ü, Reich PB, Sellin A, Shipley B, Wright IJ (2007)
672 "Diminishing returns" in the scaling of functional leaf traits across and within species
673 groups. Proc Natl Acad Sci 104:8891–8896.

674 Niklas KJ, Cobb ED, Spatz H-C (2009) Predicting the allometry of leaf surface area and dry
675 mass. Am J Bot 96:531–536.

676 Niklas K, Spatz H-C (2012) Plant Physics.

677 Normand F, Bissery C, Damour G, Lauri P-É (2008) Hydraulic and mechanical stem
678 properties affect leaf–stem allometry in mango cultivars. New Phytol 178:590–602.

679 Olson ME, Aguirre-Hernández R, Rosell JA (2009) Universal foliage-stem scaling across
680 environments and species in dicot trees: plasticity, biomechanics and Corner's Rules.
681 Ecol Lett 12:210–219.

682 Olson ME, Anfodillo T, Rosell JA, Petit G, Crivellaro A, Isnard S, León-Gómez C, Alvarado-
683 Cárdenas LO, Castorena M (2014) Universal hydraulics of the flowering plants: vessel
684 diameter scales with stem length across angiosperm lineages, habits and climates. Ecol
685 Lett 17:988–997.

686 Olson ME, Rosell JA, Zamora Muñoz S, Castorena M (2018) Carbon limitation, stem growth
687 rate and the biomechanical cause of Corner's rules. Ann Bot 122:583–592.

688 Olson ME, Soriano D, Rosell JA, Anfodillo T, Donoghue MJ, Edwards EJ, León-Gómez C,
689 Dawson T, Martínez JJC, Castorena M, Echeverría A, Espinosa CI, Fajardo A, Gazol
690 A, Isnard S, Lima RS, Marcati CR, Méndez-Alonzo R (2018) Plant height and
691 hydraulic vulnerability to drought and cold. Proc Natl Acad Sci 115:7551–7556.

692 Onoda Y, Wright IJ, Evans JR, Hikosaka K, Kitajima K, Niinemets Ü, Poorter H, Tosens T,
693 Westoby M (2017) Physiological and structural tradeoffs underlying the leaf
694 economics spectrum. New Phytol 214:1447–1463.

695 Parkhurst DF, Loucks OL (1972) Optimal leaf size in relation to environment. J Ecol 60:505–
696 537.

697 Petit G, Anfodillo T, Mencuccini M (2008) Tapering of xylem conduits and hydraulic
698 limitations in sycamore (Acer pseudoplatanus) trees. New Phytol 177:653–664.

699 Petit G, DeClerck FAJ, Carrer M, Anfodillo T (2014) Axial vessel widening in arborescent
700 monocots. Tree Physiol 34:137–145.

701 Petit G, Pfautsch S, Anfodillo T, Adams MA (2010) The challenge of tree height in
702 Eucalyptus regnans: when xylem tapering overcomes hydraulic resistance. New
703 Phytol 187:1146–1153.

704 Petit G, Savi T, Consolini M, Anfodillo T, Nardini A (2016) Interplay of growth rate and
705 xylem plasticity for optimal coordination of carbon and hydraulic economies in
706 Fraxinus ornus trees. Tree Physiol 36:1310–1319.

707 Pittermann J, Olson ME, Way D (2018) Transport efficiency and cavitation resistance in
708 developing shoots: a risk worth taking. Tree Physiol 38:1085–1087.

709 Pivovaroff A, Sack S, Santiago L (2014) Coordination of stem and leaf hydraulic conductance
710 in southern California shrubs: a test of the hydraulic segmentation hypothesis. New
711 Phytol 203:842–850.

712 Poorter H, Evans JR (1998) Photosynthetic nitrogen-use efficiency of species that differ
713 inherently in specific leaf area. Oecologia 116:26–37.

714 Poorter, Rozendaal DMA (2008) Leaf size and leaf display of thirty-eight tropical tree
715 species. Oecologia 158:35–46.

716 Price CA, Enquist BJ (2007) Scaling mass and morphology in leaves: an extension of the
717 WBE model. Ecology 88:1132–1141.

718 Reich PB, Ellsworth DS, Walters MB (1998) Leaf structure (specific leaf area) modulates
719 photosynthesis–nitrogen relations: evidence from within and across species and
720 functional groups. Funct Ecol 12:948–958.

721 Rosell JA, Olson ME (2014) The evolution of bark mechanics and storage across habitats in a
722 clade of tropical trees. Am J Bot 101:764–777.

723 Rosell JA, Olson ME, Anfodillo T (2017) Scaling of xylem vessel diameter with plant size:
724 causes, predictions, and outstanding questions. Curr For Rep 3:46–59.

725 Sack L, Holbrook NM (2006) Leaf hydraulics. Annu Rev Plant Biol 57:361–381.

726 Sack L, Scoffoni C, McKown AD, Frole K, Rawls M, Havran JC, Tran H, Tran T (2012)
727 Developmentally based scaling of leaf venation architecture explains global ecological
728 patterns. Nat Commun 3:837.

729 Scoffoni C, Chatelet DS, Pasquet-kok J, Rawls M, Donoghue MJ, Edwards EJ, Sack L (2016)
730 Hydraulic basis for the evolution of photosynthetic productivity. Nat Plants 2:16072.

731 Shipley B, Lechowicz MJ, Wright I, Reich PB (2006) Fundamental trade-offs generating the
732 worldwide leaf economics spectrum. Ecology 87:535–541.

733 Smith DD, Sperry JS, Adler FR (2017) Convergence in leaf size versus twig leaf area scaling:
734 do plants optimize leaf area partitioning? Ann Bot 119:447–456.

735 Sun Jun, Fan Ruirui, Niklas Karl J., Zhong Quanlin, Yang Fuchun, Li Man, Chen Xiaoping,
736 Sun Mengke, Cheng Dongliang (2017) “Diminishing returns” in the scaling of leaf
737 area vs. dry mass in Wuyi Mountain bamboos, Southeast China. Am J Bot 104:993–
738 998.

739 Tyree MT, Ewers FW (1991) The hydraulic architecture of trees and other woody plants. New
740 Phytol 119:345–360.

741 Tyree MT, Zimmermann MH (2002) Xylem structure and the ascent of sap, 2nd edn.
742 Springer-Verlag, Berlin Heidelberg.

743 Warton DI, Wright IJ, Falster DS, Westoby M (2006) Bivariate line-fitting methods for
744 allometry. Biol Rev 81:259–291.

745 West GB, Brown JH, Enquist BJ (1999) A general model for the structure and allometry of
746 plant vascular systems. Nature 400:664–667.

747 Westoby M, Daniel S. Falster DS, Angela T. Moles, Peter A. Vesk, Wright and IJ (2002)
748 Plant ecological strategies: some leading dimensions of variation between species.
749 Annu Rev Ecol Syst 33:125–159.

White PS (1983a) Corner's Rules in Eastern deciduous trees: allometry and its implications for the adaptive architecture of trees. Bull Torrey Bot Club 110:203–212.

White PS (1983b) Evidance that temperate east north american evergreen woody plants follow Corner's rule. New Phytol 95:139–145.

Williamson GB, Wiemann MC (2010) Measuring wood specific gravity…Correctly. Am J Bot 97:519–524.

Wright IJ, Dong N, Maire V, Prentice IC, Westoby M, Díaz S, Gallagher RV, Jacobs BF, Kooyman R, Law EA, Leishman MR, Niinemets Ü, Reich PB, Sack L, Villar R, Wang H, Wilf P (2017) Global climatic drivers of leaf size. Science 357:917–921.

Wright IJ, Reich PB, Westoby M, Ackerly DD, Baruch Z, Bongers F, Cavender-Bares J, Chapin T, Cornelissen JHC, Diemer M, Flexas J, Garnier E, Groom PK, Gulias J, Hikosaka K, Lamont BB, Lee T, Lee W, Lusk C, Midgley JJ, Navas M-L, Niinemets Ü, Oleksyn J, Osada N, Poorter H, Poot P, Prior L, Pyankov VI, Roumet C, Thomas SC, Tjoelker MG, Veneklaas EJ, Villar R (2004) The worldwide leaf economics spectrum. Nature 428:821–827.

Yang D, Niklas KJ, Xiang S, Sun S (2010) Size-dependent leaf area ratio in plant twigs: implication for leaf size optimization. Ann Bot 105:71.

Fig. 1. Habits, morphological and petiole-anatomical aspects of *C. obtusa* (Urticaceae). (a) Habits of *C. obtusa*. (b) Leaf of *C. obtusa*. (c) Petiole cross-sectional anatomy of *C. obtusa* in the middle part of the petiole. (d) Close-up of petiole constitutive tissues: pith (Pith), sclerenchyma (Scle), interfascicular parenchyma (Pint), primary xylem (XI), secondary xylem (XII), total phloem (Phlo), primary phloem (Phl), secondary phloem (PhII), cortical parenchyma (Pcor), collenchyma (Coll) and epidermis (Epi). (e) Tissues and corresponding layer masks studied. (f) "Wavy" cambium with a sub-bicyclic array of vascular bundles. Arrows represent laticiferous canals. (g) Cambial discontinuities, island-like vascular bundles and a bicyclic array of vascular bundles.

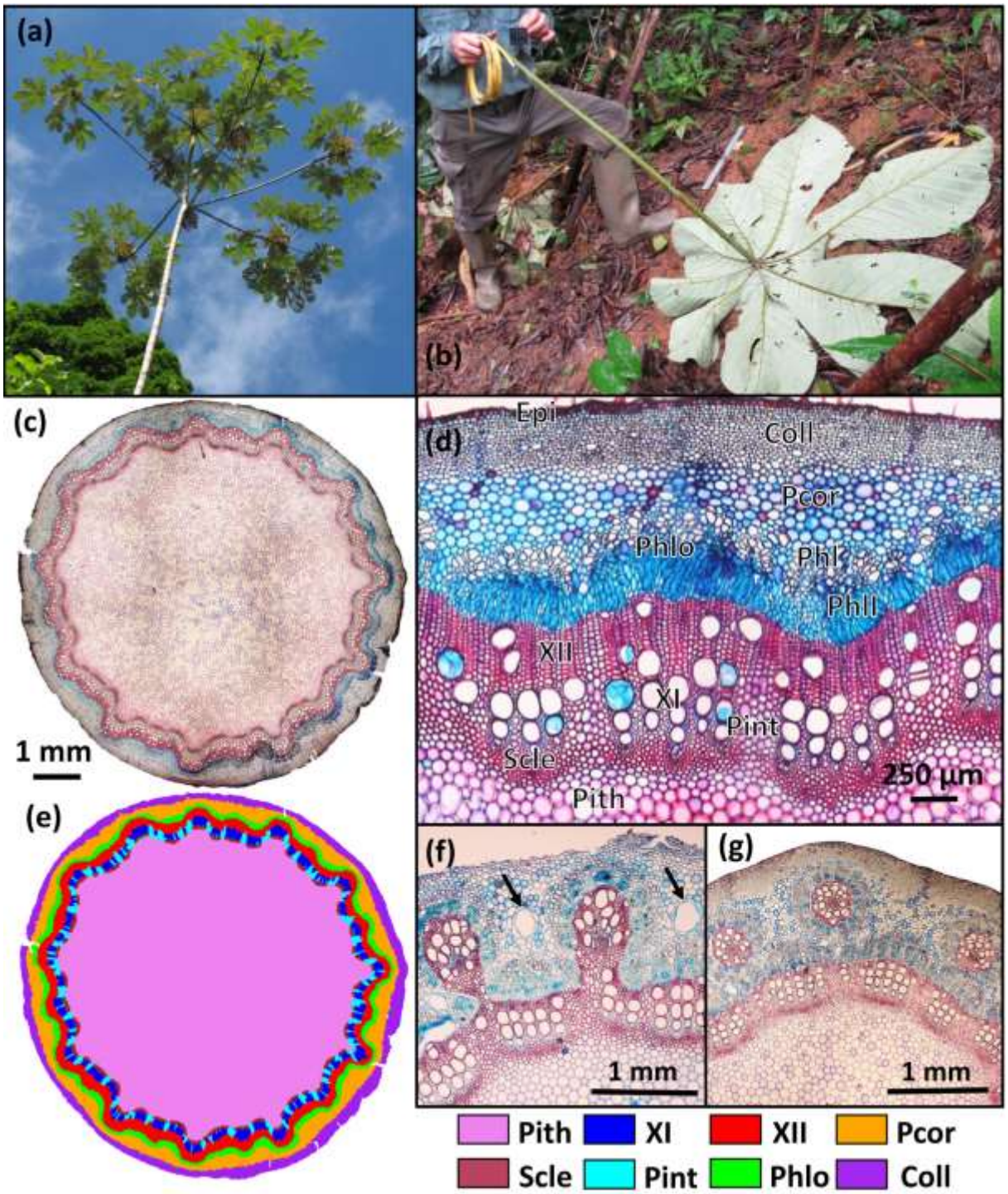

779
780
781
782
783
784
785
786

Fig. 2. Scaling of morphological traits with leaf size. (a) Lamina area according to petiole cross-sectional area. (b) Lamina dry mass according to petiole cross-sectional area. (c) Lamina dry mass according to petiole dry mass. (d) Lamina area according to leaf dry mass. All relationships are plotted on a log-scale. *b*: scaling exponent.

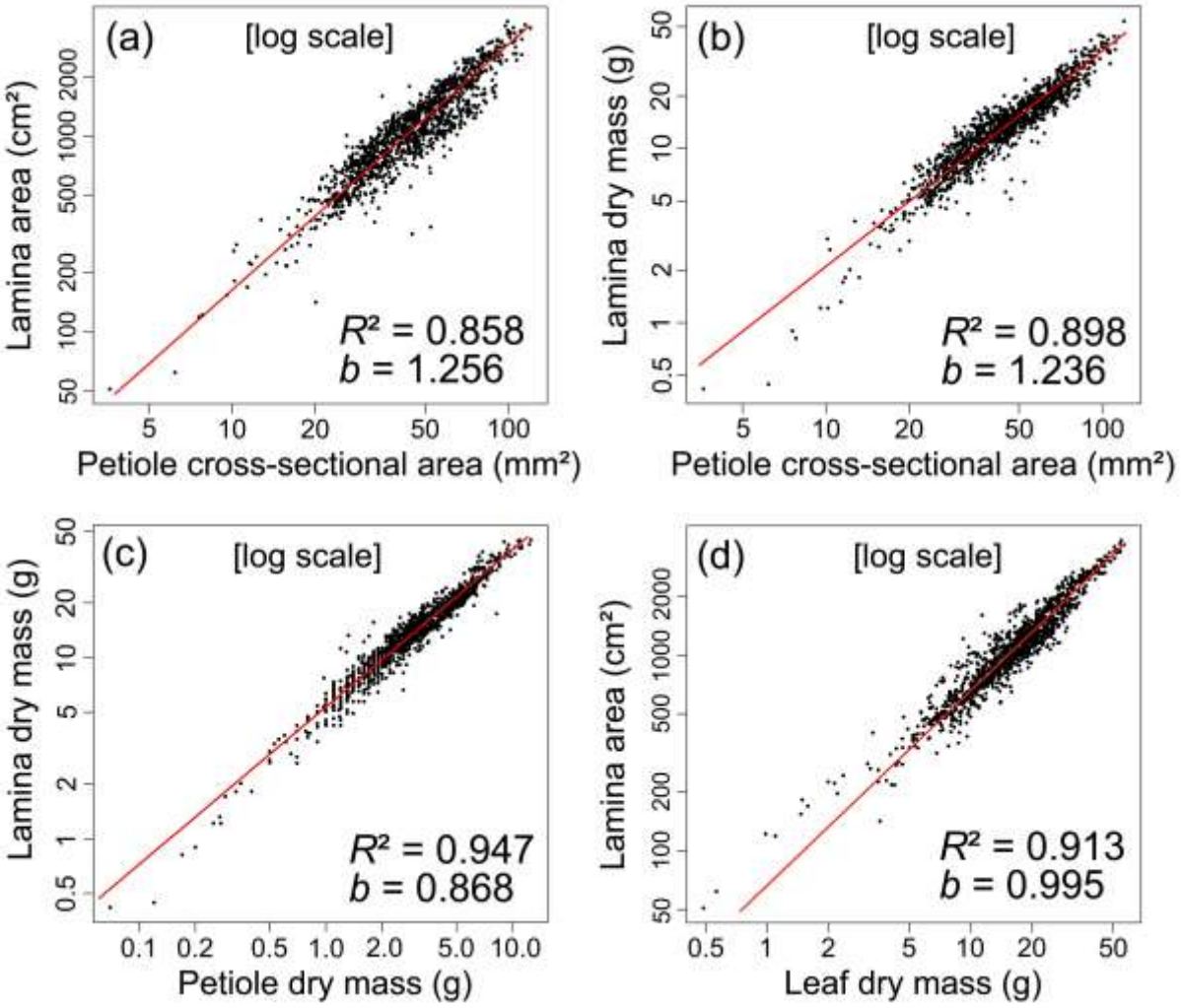

Fig. 3. Scaling of petiole anatomy with leaf size. (a) Pith cross-sectional fraction according to lamina area. (b) Number of vessels according to lamina area plotted on a log-scale. (c) Conductive area according to lamina area, plotted on a log-scale. (d) Xylem area according to lamina area, plotted on a log-scale. *b*: scaling exponent.

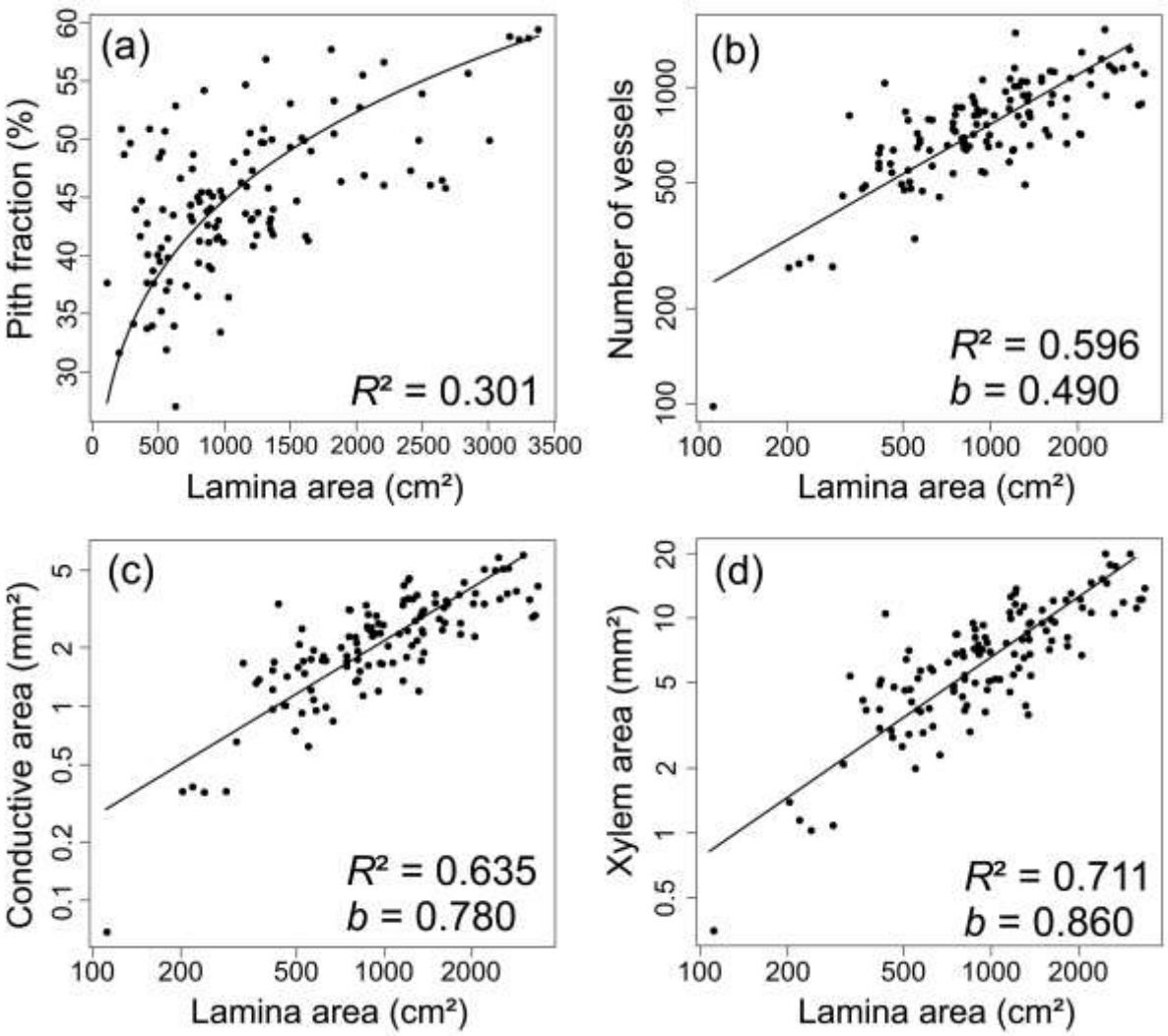

Fig. 4. Scaling of mechanical traits with leaf size. (a) Collenchyma xylem second moment of area according to lamina area. (b) Secondary xylem second moment of area according to lamina area. (c) Sclerenchyma second moment of area according to lamina area. (d) Approximated petiole flexural stiffness (product of petiole second moment of area with petiole density) according to lamina area, plotted on a log-scale. *b*: scaling exponent.

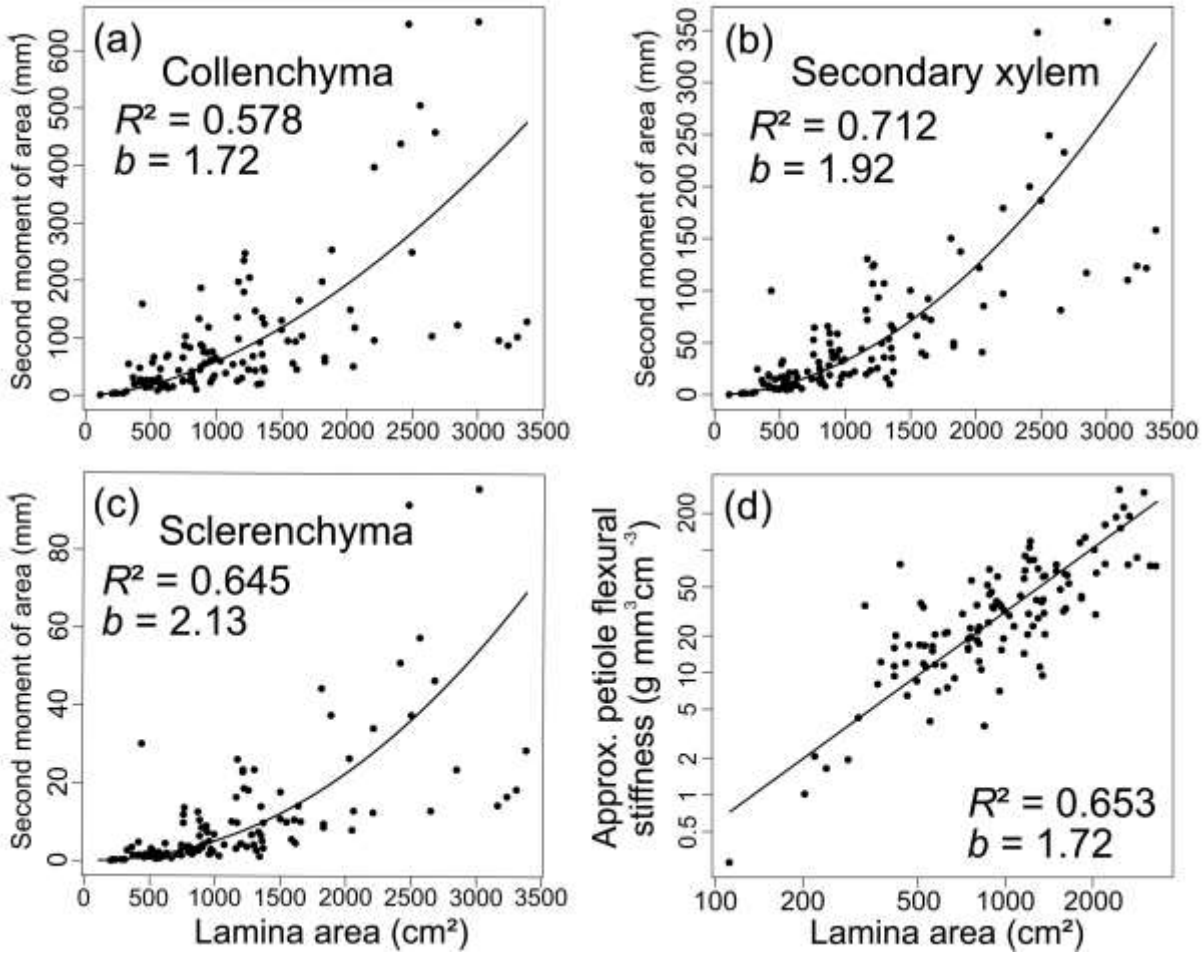

832 **Fig. 5**. Scaling of vascular traits with leaf size. (a) Mean hydraulic diameter according to
833 lamina area. (b) Mean hydraulic diameter according to path length. (c) Theoretical leaf
834 conductance under the hypothesis of no vessel widening according to lamina area. (d)
835 Theoretical leaf conductance under the hypothesis of no vessel widening according to path
836 length. All relationships are plotted on a log-scale. *b*: scaling exponent.
837

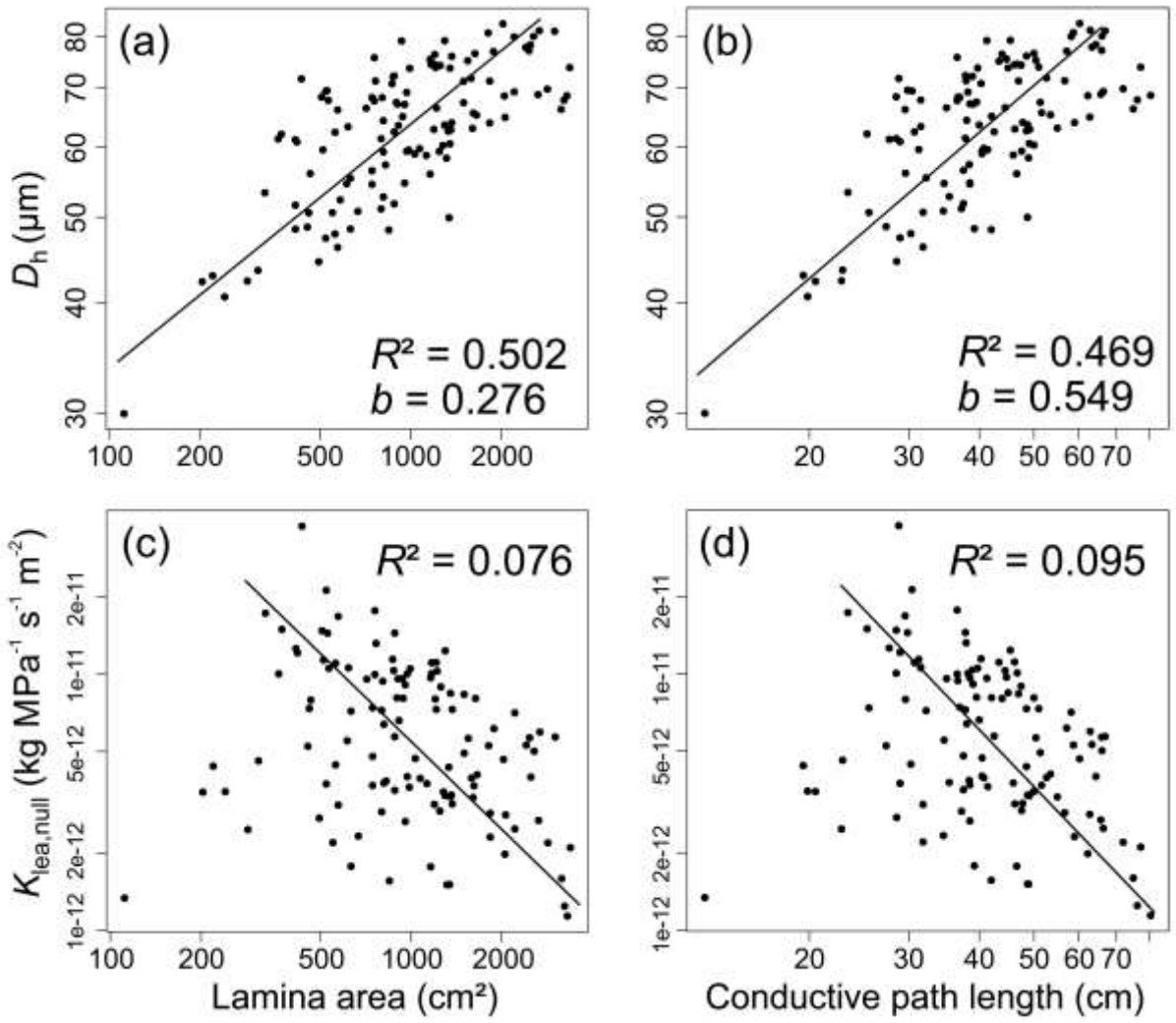

838
839

840 **Table 1**. List of measured traits and abbreviations.

841

Trait	Abbreviation	Unit	Formula
Petiole cross-sectional area	A_{pet}	mm^2	
Petiole dry mass	M_{pet}	g	
Lamina dry mass	M_{lamina}	g	
Leaf dry mass	M_{eaf}	g	$M_{leaf} = M_{petiole} + M_{lamina}$
Lamina area	A_{lamina}	cm^2	
Petiole density	PD	$g\ cm^3$	$PD = M_{dry} / (M_{fresh} - M_{immersed})$
Second moment of area of a ring-like tissue	I	mm^4	$I = pi/4*(r_{ext}^4 - r_{int}^4)$ with r_{ext} and r_{int} ring external and internal radii respectively
Approximated petiole flexural stiffness		$g\ mm^4\ cm^{-3}$	I * PD
Conductive path length	PL	cm	
Mean hydraulic diameter	D_h	µm	$D_h = (\Sigma D_v^4/N)^{1/4}$
Vessel hydraulic diameter	D_v	µm	$D_v = [32(ab)3/(a^2+b^2)]^{1/4}$ a and b major and minor ellipse diameters
Number of vessels	N_{vessel}		
Conductive area	CA	mm^2	$CA = \pi(D_h/2)^2 * N_{vessel}$
Theoretical hydraulic conductivity	K_{th}	$kg\ s^{-1}\ MPa^{-1}\ m$	$K_{th} = \Sigma K_{ellipse}$
Theoretical leaf conductance	$K_{leaf,null}$	$kg\ s^{-1}\ MPa^{-1}\ m^{-2}$	$K_{leaf} = (K_{th} / L_{pet} / 2) / A_{lamina}$
Ellipse conductivity	$K_{ellipse}$	$kg\ s^{-1}\ MPa^{-1}\ m$	$K_{ellipse} = \pi a^3 b^3/64\eta(a^3+b^3)$ with $\eta = 1.002*10^{-9}$ MPa s^{-1} at 20°C a and b major and minor ellipse diameters

842
843
844
845

846 **Table 2.** Main log-log linear relationships based on standardised major axis regression.

847

848

Y	***X***	***P***	R^2	**slope**	**95% CIs (slope)**
A_{lamina}	A_{pet}	**< 0.001**	0.858	1.256	1.229 – 1.283
M_{lamina}	A_{pet}	**< 0.001**	0.898	1.236	1.213 – 1.259
M_{lamina}	M_{pet}	**< 0.001**	0.947	0.868	0.857 – 0.881
A_{lamina}	M_{leaf}	**< 0.001**	0.913	0.995	0.977 – 1.012
D_h	PL	**< 0.001**	0.469	0.549	0.474 – 0.638
D_h	A_{lamina}	**< 0.001**	0.502	0.276	0.240 – 0.318
N_{vessel}	A_{lamina}	**< 0.001**	0.596	0.490	0.456 – 0.524
CA	A_{lamina}	**< 0.001**	0.635	0.780	0.685 – 0.875
Xylem area	A_{lamina}	**< 0.001**	0.711	0.860	0.772 – 0.978
Approx. EI	A_{lamina}	< 0.001	0.653	1.720	1.522 – 1.918

Bold values refer to significant correlation ($P < 0.05$). Table 1 for a list of abbreviations. CI: confidence interval.

849

850

851

852

853

854

855

856